IOPscience iopscience.iop.org

Home Search Collections Journals About Contact us My IOPscience

Structural and magnetic properties of Ag/Cr metallic superlattices

This article has been downloaded from IOPscience. Please scroll down to see the full text article.

1992 J. Phys.: Condens. Matter 4 5125

(http://iopscience.iop.org/0953-8984/4/22/011)

View the table of contents for this issue, or go to the journal homepage for more

Download details:
IP Address: 171.66.16.159
The article was downloaded on 12/05/2010 at 12:04

Please note that terms and conditions apply.

J. Phys.: Condens. Matter 4 (1992) 5125–5136. Printed in the UK

Structural and magnetic properties of Ag/Cr metallic superlattices

Kentaro Kyuno, Shigeki Hara, Takeo Kaneko and Ryoichi Yamamoto

Research Centre for Advanced Science and Technology, University of Tokyo, Komaba 4-6-1, Meguro-ku, Tokyo 153, Japan

Received 28 October 1991, in final form 10 March 1992

Abstract. The results of *in situ* reflection high-energy electron diffraction, x-ray diffraction, transmission electron microscopy and magnetization measurements of Ag/Cr metallic superlattices (with a few monolayers of Cr) are presented. The superlattice structure is confirmed even in the superlattice with one monolayer of Cr. It is found from simulations of the observed x-ray diffraction profiles that dramatic changes in the interplanar distances of Ag and Cr take place as a function of the number of Cr monolayers in a period. The interplanar distance of Ag contracts, whilst, on the contrary, the interplanar distance of Cr is stretched; for the superlattice which includes two monolayers of Cr it is stretched by up to about 10%. Magnetization measurements show that the magnetization per Cr atom at 5 K with an applied field of 5 T is at a maximum for two monolayers of Cr.

1. Introduction

In recent years, the novel magnetic properties predicted for ultra-thin layers of epitaxial 3d transition metals have received considerable attention. The enhanced and induced magnetic moments predicted theoretically are generally caused by the reduction of atomic coodination numbers [1–10].

Cr is one of the 3d transition metals and it is interesting because of its half-filled 3d shell. The magnetic configuration of the bulk Cr shows an incommensurate spin-density wave with a magnetic moment per atom of $0.6\mu_B$ [11–14]. Early experiments show that antiferromagnetism of bulk Cr can change drastically in thin films and fine particles [15–17]. For example Matsuo and Nishida [17] reported that single crystal particles of diameter 380–750 Å with a BCC structure showed a new magnetic transition with an ordering temperature of about 800 K. These results indicate that the anomalous behaviour should be associated with the surface. Some theories were proposed to explain these experimental results [18-22]. Teraoka and Kanamori [18] have claimed that surfaces can induce a new type of ordered magnetic structures in transition metals with a nearly half-filled d band like Cr. The idea is that for these metals the local density of states of surface atoms at the Fermi energy can be enhanced by band narrowing caused by a decrease in the number of neighbouring atoms and a transition into a more energetically stable magnetic structure occurs.

Recently, owing to new experimental developments [23–28] in the preparation and characterization of artificial materials, such as thin films, sandwiches and modulated structures, and to advances in sophisticated theoretical approaches [1–10], a number

0953-8984/92/225125+12$04.50 © 1992 IOP Publishing Ltd

of studies have been made on the ultrathin Cr films [3, 5, 6, 8–10, 29–37]. The self-consistent, spin-polarized calculations predict that the size of the magnetic moment will be enhanced by as much as 500% with respect to the bulk value in a Cr monolayer on a noble metal substrate [3, 5, 6, 8–10]. These results are explained in terms of band narrowing, as mentioned above. As for the magnetic configuration of a Cr monolayer, Blügel *et al* [5, 6] concluded that a c(2×2) antiferromagnetic configuration is energetically more stable than a p(1 × 1) ferromagnetic structure. According to their explanations the antiferromagnetic coupling of Cr seems to be a general trend.

Experimentally, Zajac *et al* [34] estimated the magnetic moment of Cr atoms at a Cr/Au(100) interface to be $2.4\mu_B$ from their UPS spectra. On the other hand, Hanf *et al* [35] find large surface moments of about $5\mu_B$ for up to three monolayers of Cr on Au(100). The experimental results for the magnetic configurations are rather controversial. Johnson *et al* [29] have performed polarized neutron reflection measurements for Ag/Cr/Ag(001) structures. For a Cr layer equivalent to the coverage of 0.33 of a monolayer, the data suggest the existence of long-range ferromagnetic order with an enhanced magnetic moment. For a layer which is 3.3 monolayers thick, no ferromagnetism was detected. Krembel *et al* [30] have performed angle-resolved photoemission measurements for a Cr monolayer on an Ag(100) surface and shown that it has a c(2 × 2) antiferromagnetic configuration.

In the present paper we report the structural and magnetic properties of Ag/Cr superlattices with a few monolayers of Cr. They were fabricated by the molecular beam epitaxy (MBE) method. The structures were investigated by *in situ* reflection high-energy electron diffraction (RHEED), x-ray diffraction and transmission electron microscopy (TEM). The magnetization was measured by a SQUID magnetometer.

The Au(001) and Ag(001) surfaces are expected to be good substrates for the epitaxial growth of BCC Cr because the atomic positions of the (001) plane of BCC Cr are almost identical to that of a (001) plane of FCC Ag and the lattice mismatch is small ($\simeq 0.2\%$). It is reported that alloying takes place at the interface in the case of the Au(001) substrate, but that no alloying takes place for the Ag(001) substrate [31, 32]. Thus the effect of interdiffusion can be removed for Ag/Cr superlattices and the intrinsic property of the Cr layer is expected to be emphasized.

2. Experimental details

The Ag/Cr superlattices were prepared by MBE. The residual gas pressure in the chamber prior to deposition was about 8×10^{-10} Torr and the pressure during deposition was 1×10^{-9} Torr. The thickness of the films and the deposition rates of Ag and Cr were measured with two quartz crystal thickness monitors. The mechanical shutters for the alternate deposition of Ag and Cr were driven using these monitors. The deposition rates of Ag and Cr were about 0.3 and 0.2 Å s^{-1}, respectively.

The (001) surface of a cleaved MgO single crystal was used as a substrate. The substrates were held on an Mo plate whose temperature was controlled by a W:Re thermocouple and a Ta heater. The substrate was cleaned at 1023 K before deposition. The first Ag layer was deposited on the substrate at 1023 K to achieve good crystalline order and the following deposition of the superlattice was started after cooling the substrate to 373 K. The thickness of the Ag layer in a period was fixed at ten monolayers and that of Cr was changed in the range of one to twelve monolayers. The overall thickness of the superlattice was taken to 1000–2000 Å.

The structure of the superlattice was investigated by RHEED during deposition, x-ray diffraction and TEM. The x-ray diffraction measurements were made using $\theta-2\theta$ diffraction with Cu Kα radiation. The instrumental resolution was estimated to be $\Delta\theta = 0.01°$. The measurements were performed with the scattering vector normal to the film plane for all superlattices. We have also measured the x-ray diffraction profile for some samples with its scattering vector not perpendicular to the film plane. The in-plane magnetization of the superlattice was measured using a SQUID magnetometer in the temperature range 5–30 K. The temperature dependence of the magnetization was measured with the applied fields kept at 5 T.

3. Results and discussion

3.1. Structure

The RHEED patterns during deposition are shown in figure 1. Figure 1(*a*) is the pattern of the MgO(001) surface before deposition. The incident direction of the electron beam is along MgO [110]. The streaks observed indicate a flat single-crystal surface. Figure 1(*b*) is the pattern after the deposition of ten monolayers of Ag and it is almost the same as that of the MgO(001) surface. This shows that the Ag layer has grown epitaxially with the same crystallographic orientation as MgO.

Figures 1(*c*) and (*d*) are the patterns after the deposition of one monolayer and three monolayers of Cr, respectively. The incident direction of the electron beam is along MgO[110]. The pattern becomes rather spotty which indicates that the surface of Cr is rougher than that of Ag (figure 1(*b*), (*f*) and (*g*)). However, the streaks still exist and Cr has grown epitaxially on Ag. The intervals of the streaks do not change and those of diffraction spots in the streak direction are stretched by up to about 40%. This suggests that the atomic positions in the Ag and Cr surfaces are the same and the interplanar distance of Ag is about 40% larger than that of Cr. This corresponds to the difference in the interplanar distance of the (001) planes of bulk Ag (2.08 Å) and bulk Cr (1.44 Å). The patterns after the deposition of four monolayers of Cr with the electron beam incident along the MgO[100] direction are also shown in figure 1(*e*). From these three figures, it is concluded that the Cr layer has a BCC structure with its (001) plane parallel to the film plane.

Figures 1(*f*) and (*g*) are the patterns of the uppermost Ag layer with the electron beam incident along the MgO[110] and [100] directions, respectively. Although the patterns are rather diffusive compared to the first layer of Ag, the streaks still exist. From these patterns, it is clear that the Ag layer has an FCC structure with its (001) plane parallel to the film plane.

In conclusion the *in situ* RHEED measurements show that the structures of the Ag and Cr layers are FCC and BCC, respectively, and that both elements have preferential growth along the [001] direction, as expected. The observed epitaxial relationships are as follows,

$$\mathrm{MgO(001)||Ag(001)||Cr(001)} \tag{1}$$

$$\mathrm{MgO[100]||Ag[100]||Cr[110]} \tag{2}$$

which are shown schematically in figure 2.

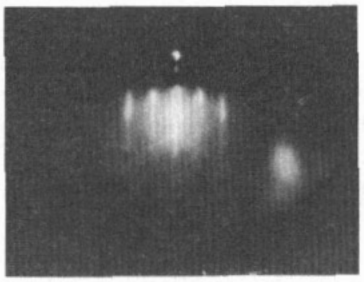

(a)

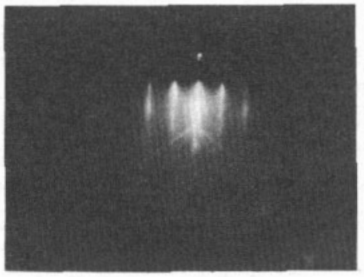

(b)

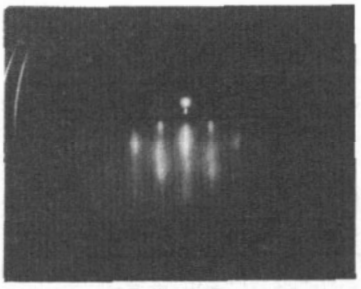

(c)

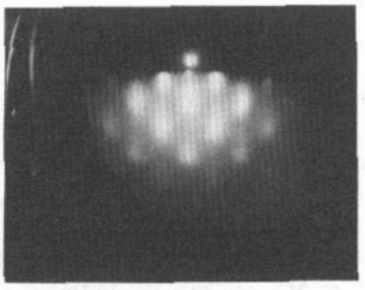

(d)

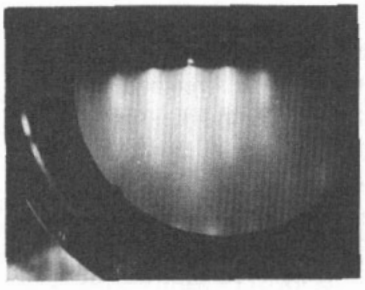

(e)

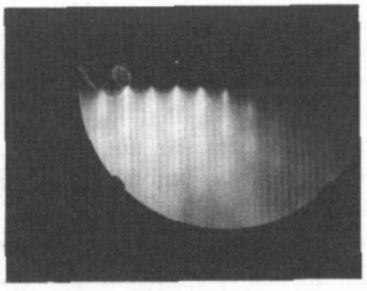

(f)

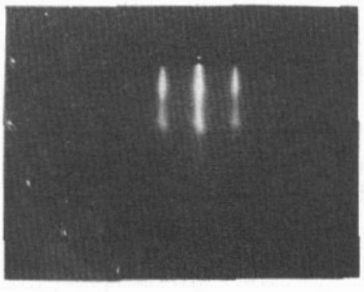

(g)

Figure 1. The RHEED patterns during deposition. The incident direction of the electron beam is (*a*)–(*d*), (*f*) along MgO[110] and (*e*), (*g*) along MgO[100]. MgO(001) surface (*a*) before deposition; (*b*) after the deposition of ten monolayers of Ag; (*c*) after the deposition of one monolayer of Cr; (*d*) after the depostion of three monolayers of Cr; (*e*) after the deposition of four monolayers of Cr; and (*f*), (*g*) the uppermost Ag layer.

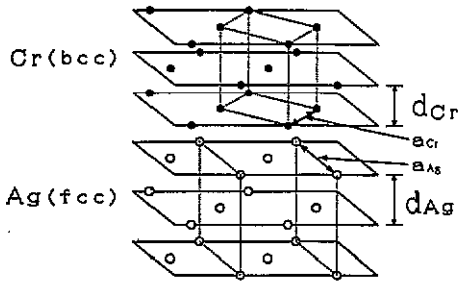

Figure 2. The schematic illustration of an Ag/Cr interface.

The x-ray diffraction profiles in the low-angle region for [Ag(10 ML)/Cr(1 ML)]$_{100}$ and [Ag(10 ML)/Cr(6 ML)]$_{87}$ are shown in figure 3. Even in the case of one monolayer of Cr, four distinct peaks are observed in the low-angle region which shows that the superlattice structure is realized. The corresponding x-ray diffraction profiles in the high-angle region are shown in figure 4 for the same samples. For [Ag(10 ML)/Cr(1 ML)]$_{100}$ six satellite peaks are observed around the main peak, which suggests that the fluctuation of the modulation wavelength is relatively small. For [Ag(10 ML)/Cr(6 ML)]$_{87}$ the satellite peaks appeared around the values of 2θ which correspond almost to the interplanar distance of the (001) planes of bulk Ag and bulk Cr and confirms relationship (1).

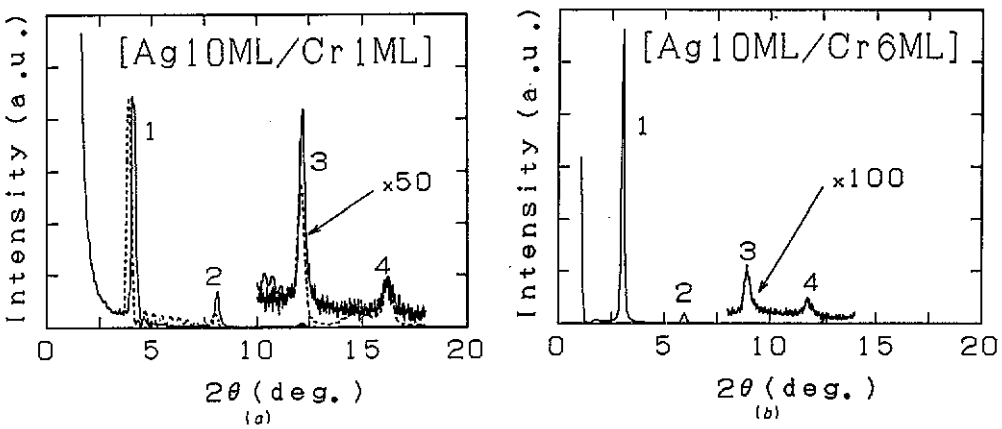

Figure 3. Measured x-ray diffraction profiles in the low-angle region of (*a*) [Ag(10 ML)/Cr(1 ML)]$_{100}$ and (*b*) [Ag(10 ML)/Cr(6 ML)]$_{87}$. The calculated profile (broken curve) is also shown for [Ag(10 ML)/Cr(1 ML)]$_{100}$.

We have estimated the interplanar distance of Ag and Cr from the observed x-ray diffraction profiles. The x-ray diffraction patterns were simulated using a model proposed by J-P Locquet *et al* [38] which takes into account the disorders due to discrete fluctuations in the number of atomic planes in each layer and continuous fluctuations of the interplanar distance, both of which have Gaussian-type distribution. We have fitted the high-angle spectra for all samples. Actually, we have considered only the discrete fluctuations in the simulations to fit the full width at half maximum of the main peak and assumed that the width of the fluctuations of Ag and Cr are

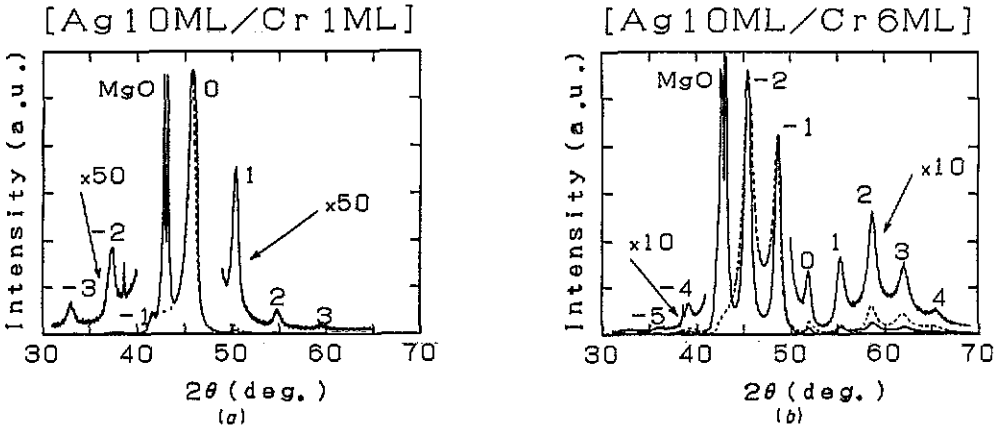

Figure 4. Measured (full curve) and calculated (broken curve) x-ray diffraction profiles in the high-angle region of (*a*) [Ag(10 ML)/Cr(1 ML)]$_{100}$ and (*b*) [Ag(10 ML)/Cr(6 ML)]$_{87}$.

the same value. The superlattice peaks should appear at the following values of θ:

$$\sin\theta = \left(\frac{2\pi n}{d} - \frac{2\pi p}{\Lambda}\right)\frac{\lambda}{2} \tag{3}$$

where n and p are running integers, d is the average of the interplanar distance, Λ is the modulation wavelength and λ the wavelength of the x-rays, respectively. So the knowledge of Λ and d obtained from the peak positions of the diffraction data give us the following set of equations:

$$\Lambda = N_{Ag}d_{Ag} + N_{Cr}d_{Cr} \tag{4}$$

$$d = \Lambda/(N_{Ag} + N_{Cr}) \tag{5}$$

where $N_{Ag}(N_{Cr})$ is the number of Ag(Cr) monolayers included in a period and $d_{Ag}(d_{Cr})$ is the interplanar distance of Ag(Cr). We assume that the interplanar distance (d_{int}) at the Ag/Cr interface is $(d_{Ag} + d_{Cr})/2$, and that $N_{Ag} = 10$, which is the value determined from the thickness monitor during growth. So we have to determine d_{Ag}, d_{Cr} and the fluctuation of $N_{Ag}(N_{Cr})$ to fit the observed profile. The calculated profiles are shown in figure 4. Figure 5 shows the values obtained for the interplanar distance of Ag and Cr as a function of the number of Cr monolayers involved in a period. The interplanar distance of Cr is stretched by up to about 10% for two monolayers of Cr and it is almost identical to the bulk value for more than five monolayers. On the contrary, the interplanar distance of Ag contracts and the change is not as large as for Cr. These results are in good agreement with those reported for Au/Cr superlattices [33]. Given the excellent lattice matching between Ag and Cr, these changes cannot be attributed to strains at the interfaces and might be caused by the change in the electronic structure.

To evaluate the validity of these results, we have fitted both the low-angle and high-angle spectra for three samples [Ag(10 ML)/Cr(1 ML)]$_{100}$, [Ag(10 ML)/Cr(2 ML)]$_{100}$ and [Ag(10 ML)/Cr(5 ML)]$_{100}$. In this case, d_{int} is also considered as a fitting parameter. The results are shown in figure 3 and figure 5. Although the fitting, which considers only the high-angle spectra and assumes $d_{int} = (d_{Ag} + d_{Cr})/2$, overestimates d_{Cr} and underestimates d_{int}, the contraction of

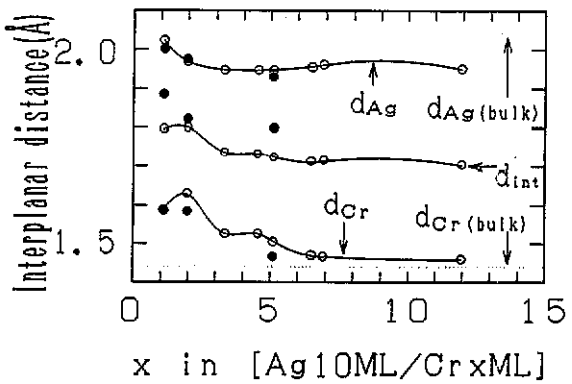

Figure 5. The interplanar distance of Ag (d_{Ag}), Cr (d_{Cr}) and the interface (d_{int}) as a function of Cr layer thickness obtained from the simulation (open circle, fitting without low-angle spectra; full circle, fitting with low-angle spectra).

d_{Ag} and expansion of d_{Cr}, especially at two monolayers, seem to be correct results. Although the value of d_{Cr} is also large for one monolayer, it is only meaningful for Cr layers which include more than one monolayer of Cr which exist because of the discrete fluctuations.

To obtain the information about in-plane structure, we performed TEM and x-ray diffraction with the scattering vector not normal to the film plane. Figure 6(*a*) shows the cross-sectional view by TEM of the [Ag(10 ML)/Cr(1 ML)]$_{100}$ superlattice. Even if the thickness of the Cr layer is one monolayer, the superlattice structure is clearly observed in the micrograph, as was indicated in the superlattice peaks of the x-ray diffraction profile.

Figure 6(*b*) shows the diffraction spots from the [Ag(10 ML)/Cr(1 ML)]$_{100}$ superlattice and the MgO substrate. The diffraction spots indicated by 'Ag' are those of the superlattice. From the positions of the spots, the interatomic distance of the superlattice in the film plane is about 3% smaller than that of MgO. This means that Ag and Cr retain their bulk interatomic distance in the film plane and that the superlattice has grown epitaxially, but not coherently, on the MgO substrate.

Figure 6(*c*) shows the diffraction spots from the [Ag(10 ML)/Cr(1 ML)]$_{100}$ superlattice alone. Since satellite peaks can be seen around each diffraction spot, the crystalline order is good not only in the perpendicular direction but also in the in-plane direction.

For some samples, we have performed x-ray diffraction measurements with the scattering vectors not perpendicular to the film plane. Figure 7 shows the contour plot of the diffraction intensity of the [Ag(10 ML)/Cr(12 ML)]$_{50}$ superlattice. Two superlattice peaks can clearly be seen beside the MgO[111] peak, which also shows that the structural order in the in-plane direction is satisfactory.

3.2. Magnetic properties

We have performed in-plane magnetization measurements on the superlattices with less than six monolayers of Cr using a SQUID magnetometer. The applied fields were 5 T at sample temperatures ranging from 5 to 30 K. Because of the very small magnetization of the superlattices, we had to subtract the magnetization of the MgO substrate for each sample. Firstly, the total magnetization of the superlattice and

(a)

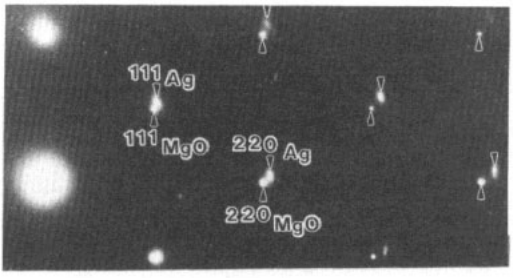

(b)

(c)

Figure 6. (*a*) The cross-sectional view by TEM of the $[Ag(10\ ML)/Cr(1\ ML)]_{100}$ superlattice. (*b*) The electron diffraction spots from the $[Ag(10\ ML)/Cr(1\ ML)]_{100}$ superlattice and MgO substrate. The diffraction spots indicated by 'Ag' are those of the superlattice. (*c*) The electron diffraction spots from the $[Ag(10\ ML)/Cr(1\ ML)]_{100}$ superlattice.

the substrate was measured. Then we used aqua regia and nitric acid to remove the superlattice from the substrate and measured the magnetization of the bare substrate which was used to evaluate the net magnetization of the superlattice. The measured magnetization of $[Ag(10\ ML)/Cr(2\ ML)]_{100}$ with the substrate and that of the bare substrate are shown in figure 8. As can be seen, the contribution from the superlattice is small—the maximum value is of the order of 10^{-4} emu. Figure 9 shows the temperature dependence of the magnetization for each sample. We assumed that Ag is not polarized and we used the Cr layer thickness evaluated from the x-ray diffraction profiles, as explained in the previous section, to calculate the magnetization of Cr. The error bars are evaluated from the difference of the two values of magnetization measured at 30 K for $[Ag(10\ ML)/Cr(1\ ML)]_{100}$, which is the largest deviation we observed. Though the error bars are rather large, it seems that the magnetizations of

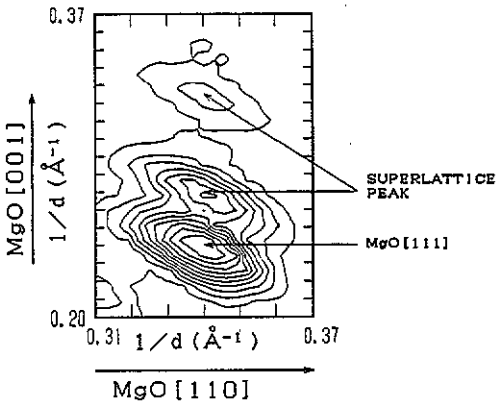

Figure 7. The contour plot of the x-ray diffraction intensity with the scattering vectors not perpendicular to the film planes for the [Ag(10 ML)/Cr(12 ML)]$_{50}$ superlattice.

the samples which include less than four monolayers of Cr increase at low temperature and those of [Ag(10 ML)/Cr(4 ML)] $_{100}$ and [Ag(10 ML)/Cr(5 ML)]$_{100}$ are almost constant at zero throughout the temperature range.

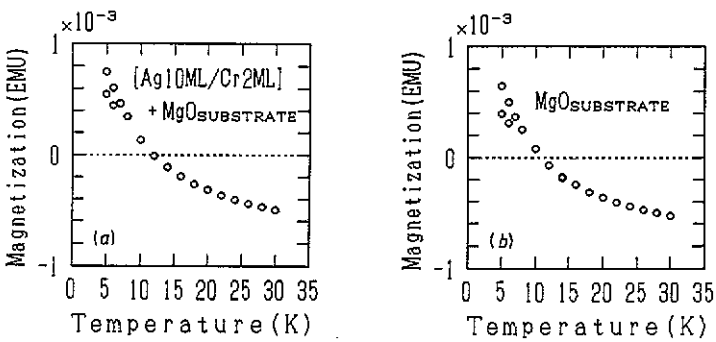

Figure 8. The temperature dependence of the magnetization of (*a*) the [Ag(10 ML)/Cr(2 ML)]$_{100}$ and MgO substrate and (*b*) the bare substrate.

We can see that the increase of the magnetization at low temperatures of [Ag(10 ML)/Cr(2 ML)]$_{100}$ is larger than those of [Ag(10 ML)/Cr(1 ML)]$_{100}$ and [Ag(10 ML)/Cr(3 ML)]$_{100}$. We have plotted $1/M$ (where M is magnetization) against temperature for [Ag(10 ML)/Cr(2 ML)]$_{100}$; the plot was reasonably linear. The deduced Curie constant leads to a value of about $1.2\mu_B$ per Cr atom, which is nearly twice the value of antiferromagnetic Cr ($0.6\mu_B$), and a Néel temperature of about 2 K. However, because of the large error bars this result should be taken as preliminary.

The origin of the smaller magnetization for a Cr monolayer than for two monolayers cannot be attributed to the difference of the magnetic moment per Cr atom because the enhancement of the magnetic moment of ultrathin layers of 3d transition metals is caused by the reduction of atomic coordination numbers. Therefore the magnetic moment of the Cr atom in a monolayer should be larger than that of the Cr atom in a double layer. The difference in the magnetization of these two superlattices can be attributed to an antiferromagnetic configuration within a monolayer. The increase of the magnetization of a Cr monolayer at low temperatures might be caused

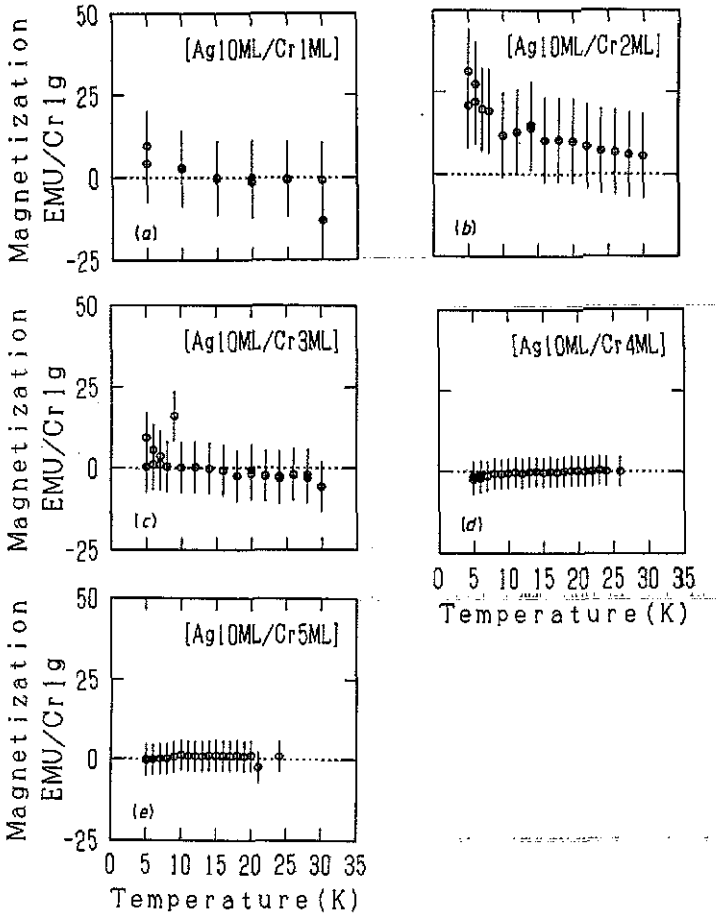

Figure 9. The temperature dependence of the magnetization for each superlattice: (*a*) $[Ag(10\ ML)/Cr(1\ ML)]_{100}$, (*b*) $[Ag(10\ ML)/Cr(2\ ML)]_{100}$, (*c*) $[Ag(10\ ML)/Cr(3\ ML)]_{100}$, (*d*) $[Ag(10\ ML)/Cr(4\ ML)]_{100}$, (*e*) $[Ag(10\ ML)/Cr(5\ ML)]_{100}$.

by the disorder of the structure. The theoretical calculations suggest that for a Cr monolayer on Ag(100), the $c(2 \times 2)$ antiferromagnetic configuration is energetically more stable than the $p(1 \times 1)$ ferromagnetic configuration [5, 6]; these are consistent with our results.

These results are contrary to the experimental data of Brodsky *et al* [37] for Au/Cr/Au sandwiches. According to their report, a Cr monolayer gave a paramagnetic susceptibility with a magnetic moment per atom ranging from 0.02 to $0.34\mu_B$, which is larger than that of two monolayers. Oguchi and Freeman [10] calculated the electronic structures of Au/Cr/Au sandwiches and concluded that the ferromagnetic Cr monolayers couple antiferromagnetically and support the results of Brodsky *et al* [37] that the magnetization of a Cr monolayer is larger than two monolayers. Their calculations assumed that a Cr monolayer is ferromagnetic, but, as mentioned above, Blügel *et al* [5, 6] also considered the antiferromagnetic configuration and concluded that it is energetically more favourable than the ferromagnetic one. So, if a calculation is made for two monolayers of Cr in which Cr is aligned antiferromagnetically within a monolayer, then it might be possible to explain why the magnetization peaks at

two monolayers and whether it has something to do with the dramatic change in the interplanar distance of Cr.

For the samples with more than three monolayers of Cr, the magnetization decreases and it seems that the antiferromagnetic configuration of the bulk Cr has already formed.

4. Conclusions

We have studied the structures and magnetic properties of Ag/Cr metallic superlattices by *in situ* RHEED, x-ray diffraction, TEM and magnetization measurements. The quality of the superlattice structure is quite satisfactory, as expected. It is revealed from the simulations of the x-ray diffraction profiles that the interplanar distance of Ag contracts and that of Cr is stretched. Surprisingly the interplanar distance of a Cr double layer is stretched by about 10%.

The magnetizations of the superlattices which include less than four monolayers of Cr increase at low temperatures and are a maximum for two monolayers. From these results we conclude that a Cr monolayer is antiferromagnetic. The superlattices which include more than three monolayers of Cr are not magnetized at low temperature and it seems that the antiferromagnetic structure of the bulk has already formed at this thickness.

Acknowledgments

We would like to thank Dr T Katayama of the Electrotechnical Laboratory for enlightening discussions and magnetization measurements. We also thank Dr Y Takahashi for the TEM observations. Work was supported by a grant-in-aid for scientific research from the Ministry of Education, Science and Culture, Japan under grant no. 02254103.

References

[1] Freeman A J 1980 *J. Magn. Magn. Mater.* **15–18** 1070
[2] Fu C L, Freeman A J and Oguchi T 1985 *Phys. Rev. Lett.* **54** 2700
[3] Freeman A J and Fu C L 1987 *J. Appl. Phys.* **61** 3356
[4] Richter R, Gay J G and Smith J 1985 *Phys. Rev. Lett.* **54** 2704
[5] Blügel S, Weinert M and Dederichs P H 1988 *Phys. Rev. Lett.* **60** 1077
[6] Blügel S, Drittler B, Zeller R and Dederichs P H 1989 *Appl. Phys.* A **49** 547
[7] Ohnishi S, Fu C L and Freeman A J 1985 *J. Magn. Magn. Mater.* **50** 161
[8] Fu C L and Freeman A J 1985 *Phys. Rev.* B **33** 4620
[9] Richter R, Gay J G and Smith J J 1985 *J. Vac. Sci. Technol.* A **3** 1498
[10] Oguchi T and Freeman A J 1986 *J. Magn. Magn. Mater.* **54–57** 797
[11] Shull C G and Wilkinson M K 1953 *Rev. Mod. Phys.* **25** 100
[12] Fawcett E 1988 *Rev. Mod. Phys.* **60** 209
[13] Slater J C 1951 *Phys. Rev.* **82** 538
[14] Asano S and Yamashita J 1967 *J. Phys. Soc. Japan* **23** 714
[15] Schmidt P H, Castellano R N, Barz H, Matthias B T, Huber J G and Fertig W A 1972 *Phys. Lett.* A **41** 367
[16] Matsuo S, Nishida I, Kimoto K and Noguchi S 1978 *J. Phys. Soc. Japan* **44** 1387
[17] Matsuo S and Nishida I 1980 *J. Phys. Soc. Japan* **49** 1005

[18] Teraoka Y and Kanamori J 1978 *Physica* B **91** 199
[19] Allan G 1978 *Surf. Sci.* **74** 79
[20] Allan G 1979 *Phys. Rev.* B **19** 4774
[21] Allan G 1981 *Surf. Sci. Rep.* **1** 121
[22] Grempel D R 1981 *Phys. Rev.* B **24** 3928
[23] Gradmann U, Bergholz R and Bergter E 1985 *Thin Solid Films* **126** 107
[24] Stampanoni A 1989 *Appl. Phys.* A **49** 449
[25] Krebs J J 1989 *Appl. Phys.* A **49** 513
[26] Rau C 1989 *Appl. Phys.* A **49** 579
[27] Dowben P A, Onellion M and Kime Y J 1988 *Scanning Microscopy* **2** 177
[28] Bauer E and van der Merve J H 1986 *Phys. Rev.* B **33** 3657
[29] Johnson A D, Bland J A C, Norris C and Lauter H 1988 *J. Phys. C: Solid State Phys.* **21** L899
[30] Krembel C, Hanf M C, Peruchetti J C, Bolmont D and Gewinner G 1991 *J. Magn. Magn. Mater.* **93** 529
[31] Hanf M C, Pirri C, Peruchetti J C, Bolmont D and Gewinner G 1989 *Phys. Rev.* B **39** 1546
[32] Hanf M C, Haderbache L, Wetzel P, Pirre C, Peruchetti J C, Bolmont D and Gewinner G 1988 *Solid State Commun.* **68** 113
[33] Bisanti P, Brodsky M B, Felcher G P, Grimsditch M and Sill L R 1987 *Phys. Rev.* B **35** 7813
[34] Zajac G, Bader S D and Friddle R J 1985 *Phys. Rev.* B **31** 4947
[35] Hanf M C, Pirri C, Peruchetti J C, Bolmont D and Gewinner G 1987 *Phys. Rev.* B **36** 4487
[36] Brodsky M B, Marikar P, Friddle R J, Singer L and Sowers C H 1982 *Solid State Commun.* **42** 675
[37] Brodsky M B, Sill L R and Sowers C H 1986 *J. Magn. Magn. Mater.* A **54–57** 779
[38] Locquet J-P, Neerinck D, Stockman L and Bruynseraede Y 1989 *Phys. Rev.* B **39** 13338